Journal of Crohn's and Colitis, 2025, **19(11)**, jjaf200
https://doi.org/10.1093/ecco-jcc/jjaf200
Advance access publication 19 November 2025
Original Article

Automated real-time imaging of intestinal barrier integrity and molecular profiling for early outcome prediction in inflammatory bowel disease: endo-histo-barrier-omics study

Marietta Iacucci*[,1], Snehali Majumder[1], Irene Zammarchi[1], Giovanni Santacroce[1], Ivan Capobianco[1], Cecilia Lina Pugliano[1], Ujwala Chaudari[2], Pablo Meseguer Esbri[3], Brian Hayes[4,5], Rory Crotty[4], Maria R. Aburto[6], Maria Rocio del Amor[3], Bisi Bode Kolawole[2], Julia Eckenberger[1], Asma Amamou[1], Valery Naranjo[3], Enrico Grisan[2], Subrata Ghosh[1], and Endo-Histo-Barrier-Omics Group

[1]APC Microbiome Ireland, College of Medicine and Health, University College Cork, Cork, Ireland
[2]School of Engineering, London South Bank University, London, United Kingdom
[3]Instituto de Investigación e Innovación en Bioingeniería, HUMAN-Tech, Universitat Politècnica de València, València, Spain
[4]Department of Histopathology, Cork University Hospital, Cork, Ireland
[5]Deparment of Pathology, University College Cork, Cork, Ireland
[6]APC Microbiome Ireland, Department of Anatomy and Neuroscience—School of Medicine, University College Cork, Cork, Ireland

*Corresponding author: Marietta Iacucci, APC Microbiome Ireland, College of Medicine, and Health, University College Cork, Consultant Gastroenterologist—Mercy/Cork University Hospitals, Room 1.07 Clinical Sciences Building CUH, Cork, Ireland (miacucci@ucc.ie).

Author Contributions: Snehali Majumder and Irene Zammarchi contributed equally.

Abstract

Background: Barrier healing is an emerging therapeutic target in inflammatory bowel disease (IBD), though its assessment remains challenging. We evaluated automated advanced imaging for real-time barrier assessment, its correlation with epithelial/vascular barrier markers, and ability to predict adverse outcomes.

Methods: IBD patients and healthy controls undergoing endoscopic assessment were prospectively enrolled. The intestinal barrier was evaluated using ultra-high-magnification endocytoscopy and probe-based confocal laser endomicroscopy. Targeted biopsies were obtained from inflamed and non-inflamed segments. Epithelial and vascular barriers were assessed through automated multiplex immunofluorescence for Claudin-2, ZO-1, E-cadherin, PV-1, and CD31. Gene expression profiling was performed in epithelial and lamina propria compartments. Artificial intelligence (AI)-based analysis was employed for automated evaluation of barrier features captured by advanced imaging.

Results: In total, 103 patients were included (38 ulcerative colitis [UC], 54 Crohn's disease [CD], 11 healthy controls). Advanced imaging revealed barrier healing in 21% (8/38) of UC and 30% (16/54) of CD patients. In UC, Claudin-2 moderately correlated with abnormal crypt architecture ($\rho = 0.49$), goblet cell depletion ($\rho = 0.5$), and overall endocytoscopy activity ($\rho = 0.49$). In CD, PV-1 moderately correlated with altered blood flow ($\rho = 0.41$) and vessel architecture ($\rho = 0.40$). An integrated assessment of advanced imaging, combined with Claudin-2 and PV-1 expression, effectively predicted adverse outcomes in UC and CD, respectively. AI tools accurately classified epithelial and vascular barrier features captured by advanced imaging. Finally, gene expression confirmed upregulation of Claudin-2 and PV-1 in IBD.

Conclusion: Automated advanced imaging enables real-time barrier assessment in IBD and correlates with markers of epithelial and vascular barrier impairment. AI integration can enhance standardization toward broader clinical applicability.

Key words: artificial intelligence; advanced imaging; barrier impairment; Claudin-2; gene expression; multiplex immunofluorescence; PV-1

Graphical Abstract

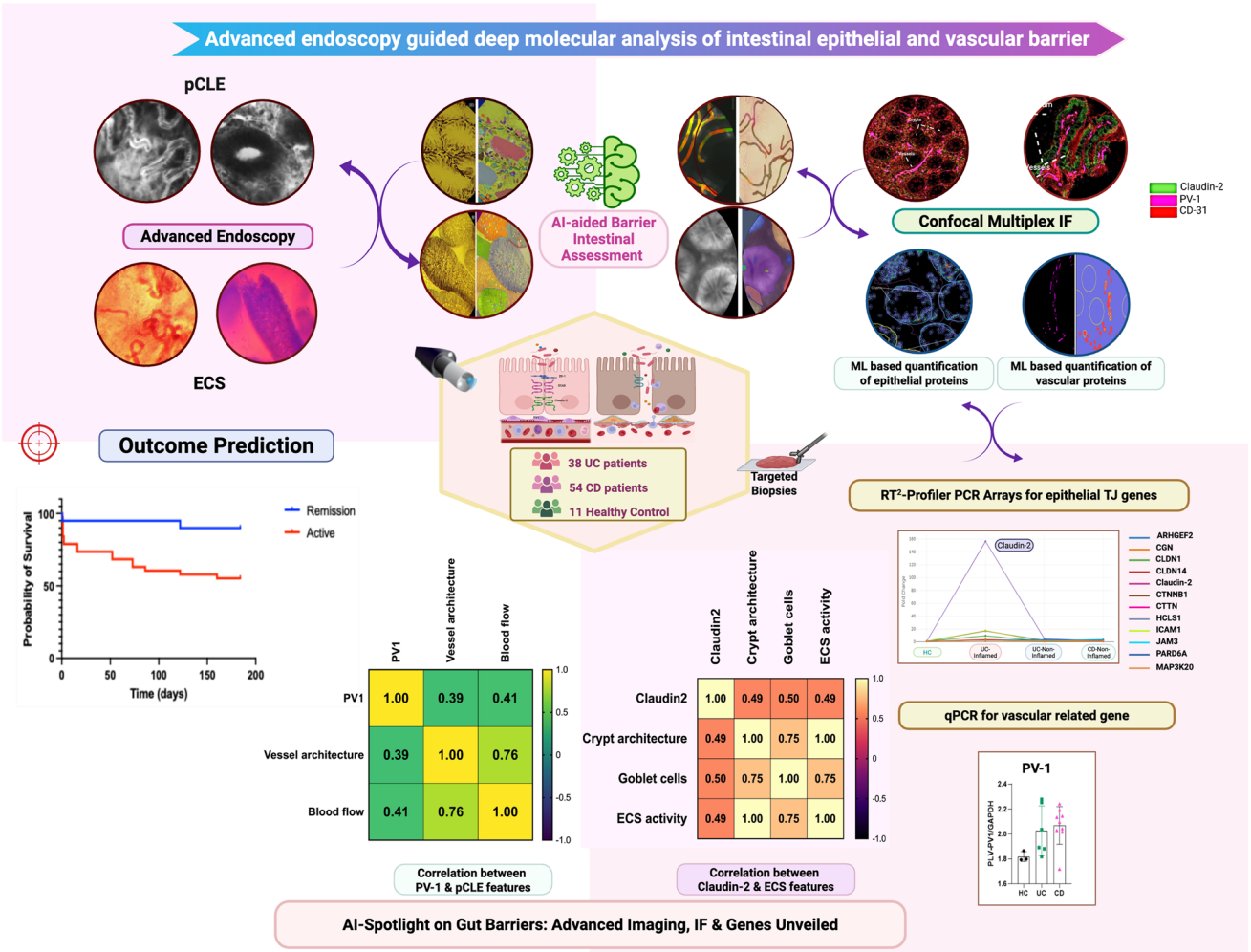

1. Introduction

The intestinal barrier, comprising epithelial and vascular components, is increasingly recognized as a key player in the onset and progression of inflammatory bowel disease (IBD).[1] Beyond its role in disease pathogenesis, barrier healing has recently emerged as a promising therapeutic target, with growing interest in developing novel drugs capable of restoring the intestinal barrier.[1,2] Recent evidence suggests that patients achieving barrier healing experience better outcomes compared to those who reach only endoscopic or histological remission.[3]

Nonetheless, until recently, assessing barrier integrity has remained challenging. Conventional endoscopy and standard histology are limited in their ability to detect structural and functional barrier dysfunction.[4] Alternative diagnostic approaches, such as probe-based assays, lack specificity and validation. Although *in vitro* assessments of epithelial and vascular proteins, including Claudin-2, occludin, JAM-A, and plasmalemma vesicle-associated protein-1 (PV-1),[5,6] are considered a more accurate option, they are technically demanding, require advanced expertise, and are not applicable for real-time clinical decision-making.

Recent advances in ultra-high-magnification endoscopic imaging, including probe-based confocal laser endomicroscopy (pCLE) and endocytoscopy (ECS), provide real-time, *in vivo* visualization of epithelial and vascular architecture.[7] These tools enable minimally invasive assessment of the intestinal barrier, allowing detailed evaluation of intestinal crypts and villi architecture, goblet cells, cell infiltration, as well as dynamic vascular architecture and blood flow. Furthermore, pCLE can reveal fluorescein leakage, which reflects functional impairment of the intestinal barrier. Early data suggest that ECS- and pCLE-based barrier evaluation may predict adverse clinical outcomes in IBD.[3,8] However, their widespread adoption is hindered by the need for specialized expertise and significant interobserver variability, though the technology is relatively straightforward. Artificial intelligence (AI) has the potential to overcome these limitations by enabling objective, standardized, and reproducible assessment of intestinal barrier healing.[9,10] Yet, evidence supporting the use of AI-enabled barrier imaging assessment remains scant. Moreover, comprehensive characterization of barrier-related gene expression in IBD is crucial to advance our understanding of disease pathogenesis, discover predictive biomarkers for disease progression and guide targeted therapeutic development.[11,12]

Based on this rationale, the present study aimed to: (1) evaluate intestinal epithelial and vascular barrier integrity using pCLE and ECS in a prospective exploratory cohort of IBD patients; (2) correlate endoscopic imaging findings with molecular barrier markers assessed through automated confocal

multiplex immunofluorescence; (3) evaluate the predictive value of pCLE and ECS combined with barrier proteins for forecasting the short-term clinical outcomes; (4) develop a novel AI model to automate and standardize advanced endoscopy-driven barrier assessment; and (5) assess the expression of barrier-related genes to support disease-specific molecular characterization.

2. Material and methodology

We conducted a prospective, observational, exploratory study at two tertiary referral IBD centers in Cork, Ireland: Cork University Hospital and Mercy University Hospital. The study received ethical approval from the Clinical Research Ethics Committee of Cork Teaching Hospitals (CREC), under references ECM 3(u) and ECM 3(1), dated December 5, 2023 (Study codes APC-159 and APC-180). Informed consent was obtained from all participants.

2.1. Study population and design

This study included adult patients aged 18-75 years with a confirmed diagnosis of IBD—either ulcerative colitis (UC) or Crohn's disease (CD)—who underwent colonoscopy for disease assessment or surveillance between March 2023 and May 2025. Healthy controls (HCs) were recruited among patients undergoing colonoscopy for cancer screening or evaluation of gastrointestinal symptoms with no history of gastrointestinal or systemic inflammatory disease, no active medication use, and showing normal endoscopic and histologic findings.

2.2. Baseline data collection and follow-up

At the baseline procedure, demographics and clinical data were collected. All patients underwent advanced endoscopic procedures for grading inflammation and to evaluate real-time "*in vivo*" intestinal barrier assessment. Targeted intestinal biopsies were obtained in the same area assessed by advanced imaging for histological analysis, evaluation of the molecular barrier, and gene expression profiling. Patients were followed for up to 12 months to monitor early clinical major adverse outcomes (MAOs).

2.3. Endoscopic assessment

Endoscopic examinations were performed using high-definition white light endoscopy and virtual chromoendoscopy, including iScan and optical enhancement (Pentax, Tokyo, Japan), as well as narrow band imaging, texture and color enhancement imaging, and red dichromatic imaging (Olympus, Tokyo, Japan). Disease activity was scored using the Mayo Endoscopic Score (MES), Ulcerative Colitis Endoscopic Index of Severity (UCEIS), and Paddington International Virtual Chromoendoscopy Score (PICaSSO) for UC, and the Simple Endoscopic Score (SES-CD) for CD. Endoscopic remission was defined as MES < 1 and UCEIS ≤ 1 for UC, and SES-CD < 3 for CD. All procedures were conducted by experienced endoscopists (M.I., S.G.) and systematically video recorded. Endoscopic findings were additionally scored by other IBD-experienced investigators (I.Z., G.S., I.C., C.P.) during the procedure.

2.4. Advanced endoscopic imaging barrier assessment

In vivo assessment of the intestinal barrier was conducted using advanced imaging modalities, including ultra-high-magnification ECS or pCLE, depending on hospital availability. ECS employed a high-resolution integrated endocytoscope, enabling ultra-high magnification of the mucosal surface at the push of a button on the endoscopy handle. pCLE was conducted with a dedicated miniprobe introduced through the working channel of the endoscope. For pCLE, intravenous fluorescein sodium (2.5-5 mL of 10% solution) was administered immediately before imaging to provide contrast and enable visualization of cellular and microvascular structures. Barrier integrity was classified into three levels: healing, mild impairment, and moderate to severe impairment, based on modified scoring systems from our prior work.[8,11] Examination details, scoring criteria, and barrier healing definitions are provided in Supplementary Material 1 and shown in Figures 1 and 2. All procedures were video recorded and conducted by experienced IBD experts and gastroenterologists (M.I., S.G.), and agreed upon by further IBD-experienced investigators (I.Z., G.S., I.C., C.P.). Each colonic segment was assessed with advanced endoscopy, focusing on the most representative inflamed areas (those showing the highest inflammation at conventional endoscopy, if present) and on the most informative non-inflamed area (according to disease distribution at diagnosis).

2.5. Histological assessment

Following advanced imaging assessment, paired biopsies were obtained from each ileo-colon-rectal segment for disease evaluation. Additional targeted biopsies were obtained from the most representative inflamed and most informative non-inflamed areas evaluated with ECS or pCLE, and used for barrier analysis with multiplex immunofluorescence. In a subset of 12 patients, further paired biopsies were collected for gene expression analysis. Histological disease activity was assessed using the validated Robarts Histopathology Index (RHI), Nancy Histological Index (NHI), and PICaSSO Histological Remission Index (PHRI) by two expert IBD pathologists (B.H., R.C.). Histological remission was defined as RHI ≤ 3 with absence of neutrophils in the epithelium and lamina propria, NHI ≤ 1, and PHRI = 0. According to NHI, inflammation was graded as mild (NHI = 2), moderate (NHI = 3) and severe (NHI = 4).

2.6. Multiplex immunofluorescence

Fresh ileocolonic biopsies were immediately processed and embedded in OCT, and then cryosectioned using a protocol adapted from Lin and Lin.[13] To ensure specificity and reproducibility, we used multiple negative and orthogonal controls. Antibodies were validated in single-plex immunohistochemistry (see Figure S2.1) and immunofluorescence (IF), secondary-only and unstained controls were applied to assess non-specific signal and autofluorescence, and single-fluor controls were used for bleed-through correction.[12,14] These measures confirmed that multiplex IF signals reflected specific antigen detection. Multiplex Set-1 included Claudin-2 (1:200), PV-1 (1:500), and CD31 (1:150), and Multiplex Set-2 included ZO1 (1:150) and E-cadherin (1:150). Primary antibodies were incubated overnight at 4 °C, followed by secondary antibody incubation (1:200). Images were acquired using an Olympus EVIDENT FV3000 confocal microscope. Validation by immunohistochemistry is detailed in Supplementary Material 2.

2.7. Automated semi-quantitative estimation of TJ protein expression

Epithelial and vascular protein expression from ileal and colonic biopsies was semi-quantitatively analyzed using Qu

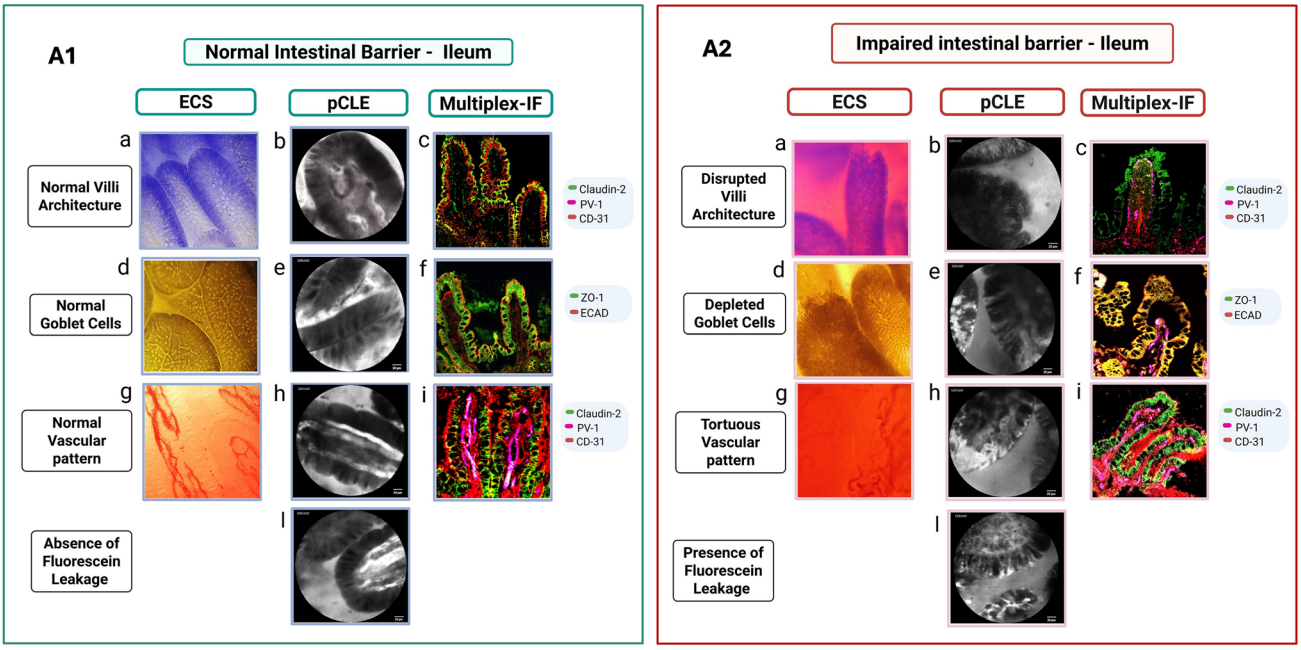

Figure 1. Multimodal imaging of normal vs impaired intestinal epithelial and vascular barrier using pCLE, ECS, and confocal multiplex immunofluorescence (mIF) in ileum. Panels A1 and A2 show ileal mucosa under normal (A1) and impaired (A2) conditions. Normal mucosa (A1) displays intact villi, goblet cells, and linear capillaries without leakage of fluorescein. mIF reveals disorganized Claudin-2, PV-1, and CD-31 patterns and loss of continuous ZO-1/E-cadherin signaling, consistent with loss of barrier integrity (A2). All mIF images were acquired at 20×.

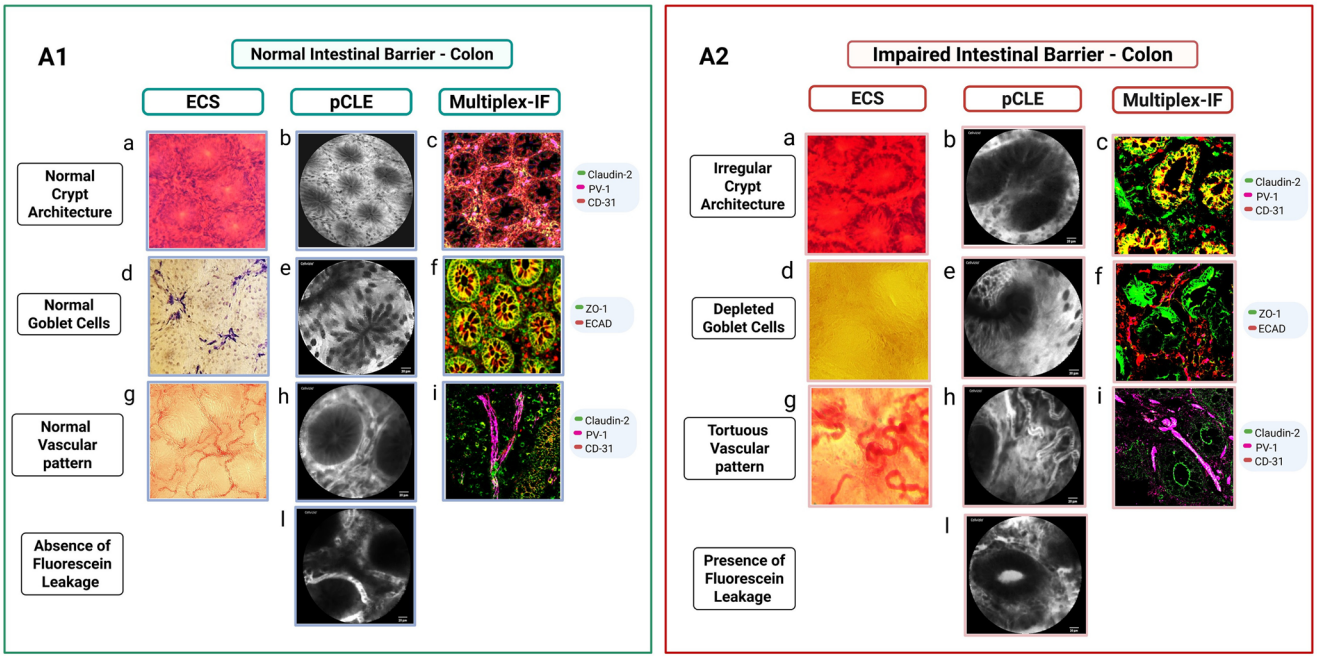

Figure 2. Multimodal imaging of normal vs impaired intestinal epithelial and vascular barrier using pCLE, ECS, and confocal multiplex immunofluorescence (mIF) in colon. Panels A1 and A2 compare normal (panels A1) and impaired (panels A2) colonic mucosa. Normal colonic mucosa (A1) shows structured crypts with intact goblet cells and preserved vascular loops without fluorescein leakage. Impaired mucosa (A2) exhibits crypt distortion, goblet cell loss, and tortuous vessels with fluorescein leakage. mIF demonstrates Claudin-2 upregulation, fragmented PV-1/CD-31 networks, and disrupted ZO-1/E-cadherin. All mIF images were acquired at 20×.

Path 0.5.1. Images were annotated into epithelium, crypts, and lamina propria. For tight junction (TJ) proteins, only epithelial and crypt regions were analyzed. Blood vessel detection used an ANN_MLP-trained pixel classifier. Protein expression thresholds were calibrated using negative controls and non-inflamed tissues to define physiological baseline levels, enabling the exclusion of background and the separation of high-intensity signals associated with inflammation-induced upregulation: 16 for Claudin-22, and 50 for CD31, PV-1, E-cadherin, and ZO-1. Cells exceeding these thresholds were considered positive. Manual adjustments were made per channel to maintain consistent quantification across samples and

minimize batch effects. Validation across representative regions ensured reproducibility and minimized user bias, consistent with best practices in digital pathology.[15,16]

2.8. AI for endoscopy automated barrier assessment

Quantitative image analysis was performed on extracted frames using AI-based models for segmentation and detailed morphometric assessment.

2.8.1. Endocytoscopy

A convolutional-neural network model based on ResNet50 architecture was trained to segment villi and crypts. Morphometric parameters, including villi and crypt area, eccentricity, diameter, and density, were automatically extracted and validated against manually annotated datasets. Additional segmentation pipelines were developed using the Segment Anything model (SAM 2.1) by META/Facebook to identify vessels and detect goblet cells, enabling the extraction of vascular and epithelial structural metrics. These included: normality vs necrosis for villi and crypts; density, tortuosity, length, and diameter for vessels; and quantification of goblet cells.

2.8.2. pCLE

Similarly, a set of annotated mosaic images was used to fine-tune a convolutional neural network (CNN) model to detect villi and crypts. The model was then applied to each frame of the available videos of colon segments to identify visible crypts, identify finger-like villi, and detect fluorescein leakage. Crypt distribution along the mucosal surface, finger-like villi, crypt/villi area, eccentricity, diameter, inter-crypt and inter-villi distance, wall thickness, and fluorescein leakage through the colonic and ileum mucosa were computed. Similarly, vessels were annotated, and average vessel density and vessel width were automatically quantified from the annotated images.

Videos were split into a training set (80% of each frame set) and a validation set (20% of each frame set), using patient-level stratification, to ensure that all the frames from a given patient (including those with multiple segments) were included in the same subset. The most predictive features, related to disease activity, such as villi, crypt architecture, leakage, and vessels, were selected based on their performance in the training set and subsequently applied to the test set.

Details of model development are provided in Supplementary Material 1.

2.9. Gene expression profiling

As proof-of-concept, a subset of patients (four UC, five CD, and three HC) was selected for transcriptomic profiling based on RNA integrity, availability of matched endoscopic imaging, histology, and intestinal barrier assessment, as well as for balanced representation of both disease phenotypes (UC and CD) and inflammatory state (inflamed and non-inflamed mucosa). This analysis was exploratory and conducted in a small, well-characterized cohort to identify molecular pathways potentially associated with epithelial and vascular barrier integrity. Therefore, gene expression profiling was performed for epithelial junction and vascular barrier proteins. Epithelial and lamina propria fractions were enzymatically separated from fresh biopsies using a protocol adapted from Booth et al.[17]

Gene expression profiling of epithelial cell junction proteins was assessed using a PCR array, which includes 84 key genes involved in TJs, adherens junctions, desmosomes, and gap junctions. Quantitative real-time PCR (qPCR) was performed to assess the expression of vascular barrier genes, including CD31, VCAD and PV-1. For full details on the extraction protocol, reverse transcriptase protocols, and details of primers used, see Supplementary Material 2.

2.10. Clinical adverse outcomes

Clinical MAOs assessed during follow-up included: colectomy due to refractory IBD (excluding cases due to dysplasia/cancer), IBD-related hospitalization, steroid initiation, treatment escalation, or modification due to persistent inflammation. Outcomes were prioritized as follows: colectomy, hospitalization, steroids, treatment change, treatment optimization. Only the first clinical MAO occurring during follow-up was used for survival analysis.

2.11. Statistical analysis

2.11.1. Technical considerations

A *P*-value of <.05 was considered statistically significant. Statistical analysis was performed with GraphPad v.10.3.1.

2.11.2. Descriptive statistics

Continuous variables were described in terms of means (SD) or median (IQR) in agreement with the Gaussian distribution (Kolmogorov–Smirnov test). Categorial variables were described in percentages and 95% CI when corresponding.

2.11.3. Comparison analysis

Mean expression was calculated on a per-biopsy basis. Normality was assessed visually using quantile–quantile plots and statistically via the Kolmogorov–Smirnov test. Comparisons of log-transformed mean protein expression were performed using the Mann–Whitney U test for two-group comparisons and the Kruskal–Wallis test for three or more groups.

2.11.4. Correlation analysis

Associations between numerical variables and log-transformed mean expression levels were analyzed using Spearman correlations.

2.11.5. Survival free from adverse outcomes

Kaplan–Meier curves for survival free from adverse outcomes were plotted and compared through the log-rank test.

2.11.6. Diagnostic performance of the model

The diagnostic performance of the AI-enabled automated barrier assessment was reported as sensitivity, specificity, positive predictive value (PPV), negative predictive value (NPV), accuracy, and F1 score. The 95% CIs for each metric were calculated.

3. Results

3.1. Population characteristics

Details about the study population are reported in Table 1. A total of 103 patients were considered: 38 (37%) with UC, 54 (52%) with CD, and 11 (11%) healthy controls (HC). Overall,

Table 1. Patients' and disease characteristics.

	UC	CD	HC
Diagnosis	38	54	11
Age (years), median (IQR)	46 (39-53)	43 (36-54)	47 (44-56)
Female sex, *N* (%)	14 (36.8)	21 (38.9)	7 (63.6)
Duration (years), median (IQR)	8 (4-13)	12 (6-20)	NA
Disease extension			
Extensive UC (%)	21 (55.3)	NA	NA
Left-sided UC (%)	13 (34.2)	NA	NA
Proctitis (%)	4 (10.5)	NA	NA
Ileal CD (%)	NA	13 (24.1)	NA
Ileocolonic CD (%)	NA	14 (25.9)	NA
Colonic CD (%)	NA	27 (50)	NA
CRP > 5 mg/L (%)	16 (42.1)	15 (27.8)	0
FCP > 250 µg/g (%)	6 (15.8)	21 (38.9)	0
Clinical remission (%)	24 (63.2)	8 (14.8)	NA
Endoscopic remission			
MES 0 (% UC)	16 (42.1)	NA	NA
UCEIS ≤ 1 (% UC)	19 (50)	NA	NA
PiCaSSO ≤ 3 (%)	19 (50)	NA	NA
SES-CD < 3 (% CD)	NA	27 (50)	NA
Advanced endoscopic remission			
ECS (%)	6/21 (28.6)	14/28 (50)	7/7 (100)
pCLE (%)	2/17 (11.8)	2/26 (7.7)	2/4 (50)
Histological remission			
RHI ≤ 4 (%)	14 (36.8)	21 (39)	11 (100)
NHI ≤ 0-1 (%)	17 (44.7)	27 (50)	11 (100)
PHRI 0 (%)	14 (36.8)	21 (39)	11 (100)

Abbreviations: CD, Crohn's disease; CRP, C-reactive protein; ECS, endocytoscopy; FCP, fecal calprotecin; HC, healthy controls; IQR, interquartile range; MES, Mayo Endoscopic subscore; NHI, Nancy Histological Index; pCLE, probe-based confocal laser endomicroscopy; PHRI, PICaSSO Histological Remission Index; PICaSSO, Paddington International Virtual Chromoendoscopy score; RHI, Robarts Histopathology Index; SES-CD, Simple Endoscopic Score for Crohn disease; UC, ulcerative colitis; UCEIS, ulcerative colitis endoscopic index of severity.

150 biopsies were analyzed: 58 (38.7%) UC; 73 (48.7%) CD, and 19 (12.7%) HC.

3.2. Ulcerative colitis cohort

In total, 36.8% (14/38) of patients were females; median age was 45.5 (39-53) years. A total of 16/38 (42.1%) of patients were in endoscopic remission according to MES. Conversely, 28.6% (6/21) and 11.8% (2/17) of patients were in remission according to ECS and pCLE-based scoring systems, respectively.

3.2.1. Protein expression, disease activity and barrier impairment

Claudin-2 expression was significantly increased in patients with mild disease activity compared to those with disease remission (117.0 [66.5-213.0] vs 223.4 [134.7-572.4]; $P = .05$).

Moreover, Claudin-2 expression increased significantly from barrier integrity to mild to moderate–severe barrier impairment when assessed by ECS (85.5 [51.6-134.6] vs 116.3 [71.1-246.6] vs 194.4 [105.7-294.8]; $P = .05$). (Table S1.5). Similarly, its expression varied according to epithelial features identified by ECS, with significantly higher levels observed when crypt architecture altered (85.1 [51.6-134.6] vs 172.3 [79.9-246.6]; $P = .04$), and goblet cell depletion (79.6 [55.4-145.4] vs 194.4 [108.1-264.2]; $P = 0.02$; Table 2). In contrast, Claudin-2 expression showed no significant differences according to epithelial and vascular barrier features visualized through pCLE.

Overall, a significant moderate positive correlation was found between Claudin-2 expression and altered crypt architecture ($\rho = 0.49$; $P = .02$), goblet cell depletion ($\rho = 0.5$; $P = 0.01$), and overall ECS score ($\rho = 0.49$; $P = .02$) (Figure S1A).

No significant differences in the expression of ZO1, E-cadherin, CD31, and PV-1 were observed in relation to disease activity and barrier impairment, as assessed by high-definition endoscopy and advanced endoscopic techniques, respectively.

Details on protein expression according to overall barrier assessment by pCLE and ECS, as well as epithelial and vascular features, are detailed in Table S1.5 and Supplementary Material 3.

Table 2. Claudin-2 expression according to advanced imaging-assessed features in UC.

		pCLE		*P*-value
Crypt architecture	**Normal**	**Irregular**	**Necrosis**	
	344.4 (181.6-527.4)	220.9 (135.2-533.9)	122.3 (95.7-226.2)	.19
Goblet cells	**Normal**	**Depleted**		
	286.4 (121.0-476.5)	149.7 (95.06-228.9)		.27
Leakage of fluorescein	**Absent**	**Present**		
	321.3 (127.6-570.3)	152.5 (96.2-300.9)		.27
Blood flow	**Normal/high/low**	**Back-and-forth/stagnant**		
	286.4 (108.7-476.5)	149.7 (97.5-228.9)		.39
Vessel architecture	**Normal**	**Dilated**	**Tortuous/disrupted**	
	384.5 (289.3-544.8)	134.1 (93.8-295.6)	136.0 (95.7-206.4)	.03*
ECS				
Crypt architecture	**Normal**	**Altered**		
	85.51 (51.64-134.6)	172.3 (79.88-246.6)		.04*
Goblet cells	**Normal**	**Depleted**		
	79.55 (55.39-145.4)	194.4 (108.1-264.2)		.02*
Vascular pattern	**Normal**	**Altered**		
	99.9 (60.4-163.3)	159.4 (80.8-241.8)		.16

Abbreviations: ECS, endocytoscopy; pCLE, probe-based confocal laser endomicroscopy; *statistically significant.

Table 3. PV-1 expression according to advanced imaging-assessed features in CD.

pCLE				*P*-value
Epithelial architecture	**Normal**	**Irregular**	**Necrosis**	
	139.6 (95.4-255.4)	145.9 (102.0-238.7)	210.7 (81.2-459.1)	0.73
Goblet cells	**Normal**	**Depleted**		
	136.8 (92.6-250.0)	207.7 (108.7-420.0)		.28
Leakage of fluorescein	**Absent**	**Present**		
	370.7 (322.9-548.4)	432.7 (364.1-515.3)		.28
Blood flow	**Normal/high/low**	**Back-and-forth/stagnant**		
	372.8 (323.3-485.5)	464.7 (375.2-601.6)		.04*
Vessel architecture	**Normal**	**Dilated**	**Tortuous/disrupted**	
	359.7 (317.7-381.6)	440.4 (388.5-540.3)	478.8 (362.7-589.6)	.04*
ECS				
Epithelial architecture	**Normal**	**Altered**		
	141.7 (111.1-241.9)	146.7 (71.6-240.4)		.48
Goblet cells	**Normal**	**Depleted**		
	133.4 (104.4-251.5)	126.3 (66.4-149.2)		.31
Vascular pattern	**Normal**	**Altered**		
	413.1 (312.2-475.1)	429.7 (343.3-457.3)		.85

Abbreviations: ECS, endocytoscopy; pCLE, probe-based confocal laser endomicroscopy.

3.3. Crohn's disease cohort

In total, 38.9% (21/54) of patients were females; median age was 43 (36-54) years. According to SES-CD, 50.0% (27/54) of patients were in endoscopic remission. Conversely, 50.0% (14/28) and 7.7% (2/26) of patients were in remission according to ECS and pCLE scoring systems, respectively.

3.3.1. Protein expression, disease activity and barrier integrity

PV-1 expression increased significantly from quiescent to mild endoscopic activity (390.4 [323.4-455.6] vs 464.1 [401.3-595.0]; $P = .04$) (Table S1.6).

Notably, PV-1 expression increased significantly from quiescent to mild disease activity as assessed by pCLE (359.7 [320.0-399.1] vs 514.4 [385.3-613.8]; $P = .05$; Table 3). Similarly, its expression varied with pCLE-assessed vascular features. Specifically, higher PV-1 expression was associated with altered blood flow (372.8 [323.3-485.5] vs 464.7 [375.2-601.6]; $P = .04$) and altered vessel architecture (359.7 [317.7-381.6] vs 440.4 [388.5-540.3] vs 478.8 [362.7-589.6], $P = .04$). Overall, a moderate positive correlation was observed between PV-1 expression and both altered blood flow ($\rho = 0.41$; $P = .01$) and vessel architecture ($\rho = 0.40$; $P = .02$) (Figure S1B).

In contrast, no significant differences in PV-1 expression were found in relation to ECS-based disease activity or specific epithelial and vascular features.

No significant differences in ZO1, ECAD, CLD-2, and CD31 expression were observed according to disease activity or barrier integrity, as assessed by high-definition endoscopy and advanced endoscopic techniques, respectively.

Further details on protein expression, in relation to overall disease activity assessed by pCLE and ECS, as well as epithelial and vascular features, are provided in Table S1.6 and Supplementary Material 3.

3.4. Outcome prediction

Overall, 36 patients experienced an adverse outcome (19 with UC and 17 with CD) over a mean follow-up period of 7.5 (4.9) months.

Patients with barrier impairment, as assessed by advanced imaging (pCLE and ECS), had significantly worse outcomes compared to those in remission. This was observed in both UC (HR 3.4 [95% CI 1.3-8.8]; $P = .01$) and CD (HR 2.9 [95% CI 1.1-7.9]; $P = .04$). Protein cut-off values predictive of adverse outcome were identified for both Claudin-2 (127.6) and PV-1 (491.0).

Significantly, the integrated assessment combining advanced imaging score with Claudin-2 and PV-1 expression better predicted clinical major adverse outcomes than advanced imaging score alone in UC (HR 3.4 [1-11.7]; $P = .05$) and CD (HR 3.0 [1.0-8.7]; $P = .04$), respectively.

Survival analysis (Figure 3) revealed that barrier impairment on advanced imaging and barrier protein expression significantly stratified clinical risk. When combined with endoscopic, histologic, and protein expression endpoints, predictive performance for clinical outcomes in UC and CD was further enhanced. (Figures S2 and S3). Moreover, patients in endoscopic remission who demonstrated barrier healing, confirmed by advanced imaging and protein expression, had a significantly lower rate of severe adverse outcomes (MAOs) compared to those without barrier healing (13% vs 56%; $P = .05$). An additional stratified analysis was performed to compare the overlap among endoscopic remission, barrier healing, and molecular marker status. In the overall IBD cohort, endoscopic remission with barrier healing and CLD2 (UC) or PV-1 (CD) negativity (according to the identified cut-off predictive of outcome), and restoration of barrier integrity was associated with markedly lower incidence of adverse outcomes ($P = .05$), highlighting the clinical relevance of molecular and functional barrier recovery. (Table S1.7).

3.5. AI-powered detection evaluation of barrier integrity using advanced imaging

Table 4 presents the model performance for assessing epithelial and vascular features.

The model demonstrated good performance in detecting abnormalities in epithelial and vascular features, thereby

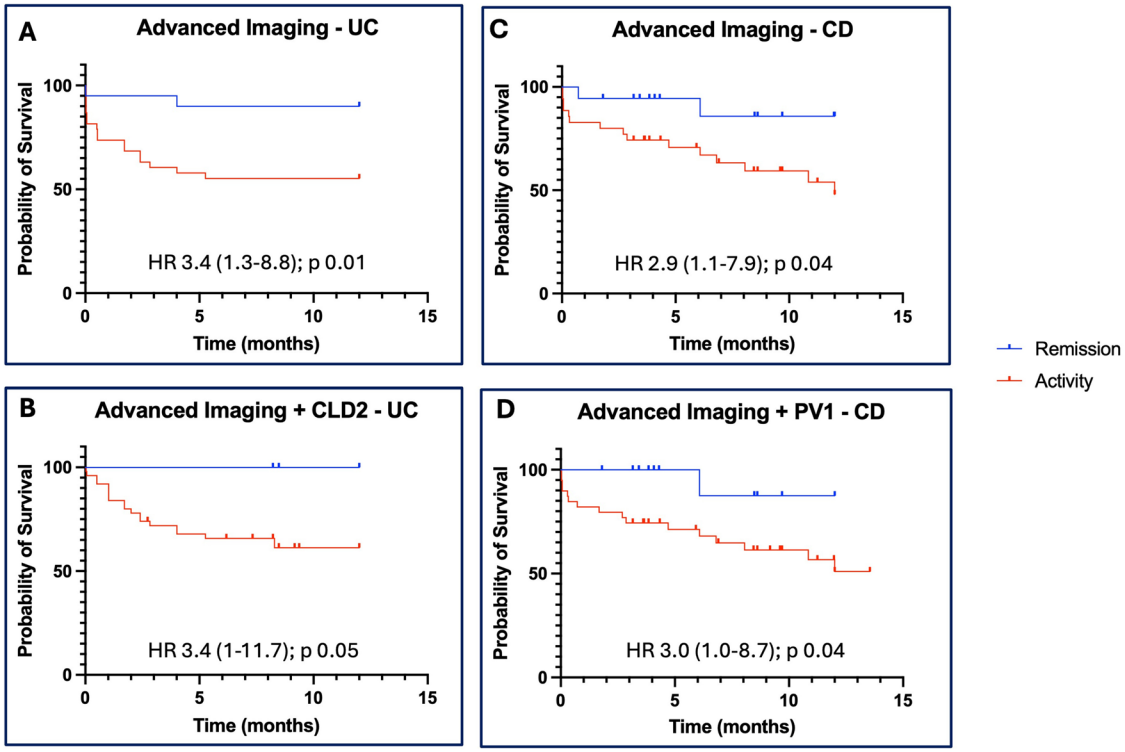

Figure 3. Kaplan–Meier curves for survival free from adverse outcomes over a 12-month follow-up according to advanced imaging activity in UC (A); advanced imaging activity combined with CLD-2 in UC (B); advanced imaging activity in CD (C); and advanced imaging activity combined with PV-1 in CD (D).

enabling accurate prediction of disease activity according to ECS and pCLE.

The model assessed the presence of villi/crypt abnormalities, vessel alteration, and goblet cell depletion by ECS with 100% (95% CI 63-100), 88% (95% CI 47-100), and 100% (95% CI 63-100) accuracy, respectively. Sensitivity was 100% (95% CI 16-100), 100% (95% CI 16-100), and 100% (95% CI 16-100), while specificity was 100% (95% CI 54-100), 83% (95% CI 36-100), and 100% (95% CI 54-100), respectively.

Similarly, the model predicted villi/crypt abnormalities, vessel alteration, and leakage of fluorescein by pCLE with 66% (95% CI 47-81), 75% (95% CI 51-91), and 74% (95% CI 60-86) accuracy; 47% (95% CI 23-72), 89% (95% CI 52-100), and 61% (95% CI 36-83) sensitivity; and 87% (95% CI 60-98), 64% (95% CI 31-89), and 83% (95% CI 64-94) specificity, respectively.

3.6. Gene expression patterns implicating intestinal barrier dysfunction

In total, 84 genes involved in epithelial barrier regulation were evaluated in nine patients (four UC and five CD). Vascular gene expression (PLV1-PV-1, VCAD and CD31) was quantified in 15 IBD patients (six UC and nine CD) and three HCs.

Transcriptomic profiling revealed pronounced dysregulation in IBD patients. Among UC patients, 55 genes were upregulated and 10 downregulated (>2-fold), while in CD, 49 genes were upregulated and four downregulated relative to HCs.

Claudin-2 was consistently upregulated (>2-fold) in ileocolonic biopsies from both UC and CD. Pathway enrichment analysis showed that tissues from IBD patients were predominantly associated with TJ-assembly and barrier organization. In contrast, HCs showed higher expression of genes associated with epithelial polarity and vascular stability.

Heatmap clustering and RT-qPCR validation further substantiated distinct expression profiles, with marked upregulation of PV-1, VCAD, and CD31 transcripts in both UC and CD, indicative of significant vascular barrier disruption.

Complete gene lists are given in Supplementary Material 2.

4. Discussion

In the evolving landscape of personalized medicine in IBD,[18] the focus of clinical trials and routine practice is increasingly shifting from traditional endoscopic and histologic endpoints toward molecular markers of mucosal healing. Barrier dysfunction is now recognized as a key contributor to IBD pathogenesis and a predictor of poor outcomes. As a result, there is growing interest in the development of therapies specifically designed to restore the integrity of the barrier.[1,7,19] However, implementing a treat-to-target strategy focused on barrier healing remains challenging, due largely to the lack of standardized, practical tools to assess barrier integrity *in vivo*.

Building on our previous studies[8,11] demonstrating the remarkable potential of ECS and pCLE to assess intestinal barrier healing and predict clinical outcomes in IBD, this exploratory study further investigated the utility of these advanced imaging modalities for real-time, *in-vivo* evaluation of barrier integrity. Moreover, we aimed to comprehensively assess the intestinal barrier by innovatively evaluating both its epithelial and vascular components. For the first time, we correlated advanced imaging-derived barrier features with automated molecular profiling of barrier-related markers. To ensure a thorough evaluation of the intestinal barrier, we selected Claudin-2, ZO-1, and E-cadherin as key epithelial barrier markers, and PV-1 and CD31 as principal vascular barrier

Table 4. Diagnostic performance of the AI model to assess abnormalities of epithelial and vascular features assessed with advanced imaging.

	ECS			pCLE			
	Crypt abnormality prediction vs activity	**Vessel abnormality prediction vs activity**	**Goblet cell depletion prediction vs activity**	**Crypt abnormality prediction vs activity**	**Ileum vessel abnormality prediction vs activity**	**Colon vessel abnormality prediction vs activity**	**Leakage score vs activity**
Accuracy (95% CI)	1.00 (0.63-1.00)	0.88 (0.47-1.00)	1.00 (0.63-1.00)	0.66 (0.47-0.81)	0.90 (0.68-0.99)	0.75 (0.51-0.91)	0.74 (0.60-0.86)
Sensitivity (95% CI)	1.00 (0.16-1.00)	1.00 (0.16-1.00)	1.00 (0.16-1.00)	0.47 (0.23-0.72)	0.94 (0.71-1.00)	0.89 (0.52-1.00)	0.61 (0.36-0.83)
Specificity (95% CI)	1.00 (0.54-1.00)	0.83 (0.36-1.00)	1.00 (0.54-1.00)	0.87 (0.60-0.98)	0.67 (0.09-0.99)	0.64 (0.31-0.89)	0.83 (0.64-0.94)
PPV (95% CI)	1.00 (0.16-1.00)	0.67 (0.09-0.99)	1.00 (0.16-1.00)	0.80 (0.44-0.97)	0.94 (0.71-1.00)	0.67 (0.35-0.90)	0.69 (0.41-0.89)
NPV (95% CI)	1.00 (0.54-1.00)	1.00 (0.48-1.00)	1.00 (0.54-1.00)	0.59 (0.36-0.79)	0.67 (0.09-0.99)	0.88 (0.47-1.00)	0.77 (0.59-0.90)
AUROC (95% CI)	1.00 (0.96-1.00)	0.93 (0.62-1.000)	1.00 (0.96-1.00)	0.77 (0.56-0.92)	0.82 (0.61-1.00)	0.78 (0.56-0.99)	0.72 (0.58-0.83)

Abbreviations: AUROC, area under the receiver operating curve; ECS, endocytoscopy; NPV, negative predictive value; pCLE, probe-based confocal laser endomicroscopy; PPV, positive predictive value.

markers, based on their established relevance to barrier integrity.[20–22] Additionally, we explored the potential of integrating advanced imaging with barrier protein profiling to accurately predict clinical MAOs accurately.

Previous studies have preliminarily investigated barrier impairment in IBD, focusing on correlation of pCLE-based leakage of fluorescein with clinical outcomes.[3,11] Fluorescein leakage first reflects vascular barrier impairment, with extravasation into the lamina propria, and, if the epithelial barrier is also compromised, can subsequently diffuse into the intestinal lumen. More recently, our group demonstrated that ECS can also evaluate the intestinal barrier, correlating with CLD-2 expression and predicting outcomes in UC. However, vascular barrier integrity has not been accurately evaluated, and imaging findings have never been correlated with molecular-level benchmarks.

Our results revealed a significant correlation between protein expression and distinct epithelial and vascular features assessed by advanced imaging techniques. Notably, Claudin-2 expression increased in UC and correlated with ECS-based barrier assessment, along with alterations in epithelial features, such as crypt architecture and goblet cell density. These findings support the established mucosal involvement in UC and show the potential utility of ECS as a novel advanced imaging tool for evaluating mucosal integrity. In contrast, PV-1 expression was significantly elevated in CD, as assessed via pCLE, and was linked to alterations in vascular features, such as vessel architecture and blood flow patterns. These results support the hypothesis that, as a transmural disease, early pathogenetic events may originate in the lamina propria and involve increased vascular permeability. They also highlight the role of pCLE in assessing vascular architecture and barrier integrity in CD.

Consistent with our previous findings,[8] we demonstrated that advanced imaging-guided barrier assessment, integrated with barrier protein profiling, can accurately predict clinical MAOs.

The combined assessment of endoscopic, histological, advanced imaging, and protein expression endpoints demonstrated remarkable predictive ability, with patients in endoscopic barrier-healing showing significantly lower rates of MAOs. This underscores the added value of combining these techniques for real-time evaluation of deep healing and personalized disease management.

Advanced endoscopic techniques remain limited to research settings, as their interpretation demands substantial expertise and is hindered by considerable interobserver variability even among experts. To address this, we have developed the first AI model designed to standardize barrier assessment using advanced endoscopy imaging. This model automatically quantifies key critical features of barrier structure and function, including villi/crypt architecture, goblet cell depletion, and vascular morphology. A key innovation in our study is the development of the first AI model to standardize the evaluation of epithelial and vascular barrier integrity from ECS and pCLE imaging. This model addresses the need for specialized expertise [11] and extends our previous work by applying automated image analysis to novel epithelial and vascular features. Our AI system demonstrated remarkable performance in identifying and quantifying villi, crypt architecture, goblet cell depletion, and vascular pattern. By enabling objective and reproducible analysis, AI represents a further step toward implementing barrier assessment as a therapeutic target in IBD.[23,24] Moreover, AI-driven standardization may enable consistent endpoint

evaluation in clinical trials and support broader integration of barrier assessment into routine care.[25]

Finally, preliminary genomic profiling confirmed the upregulation of Claudin-2 and PV-1 in IBD patients. Although small, the cohort was well-characterized to identify molecular pathways potentially associated with epithelial and vascular barrier integrity, including a balanced representation of both disease phenotypes (UC and CD) and inflammatory states (inflamed and non-inflamed mucosa). These results highlight the feasibility of integrating molecular data and provide a foundation for large-scale prospective transcriptomic studies to delineate the molecular drivers of barrier dysfunction in IBD.

Our study has certain limitations, despite offering important insights and laying the groundwork for future research. The relatively small sample size may limit generalizability, and the imbalance between UC and CD cohorts warrants further validation. Nevertheless, our prior work has already shown signals of intestinal protein expression in UC,[8] making new data on CD particularly valuable. Larger, more balanced prospective studies are underway to validate and extend these findings. Advanced endoscopy extends procedure time and requires substantial expertise, limiting routine clinical use. Its current scoring systems are also complex, designed to capture multiple facets of epithelial and vascular integrity. Our AI model standardizes the procedure and image analysis, potentially improving reproducibility and overall feasibility. Our molecular validation focused on a selected panel of epithelial and vascular barrier proteins, building on prior findings that warrant a more comprehensive proteomic and functional analysis to elucidate barrier dysfunction in IBD. Although still in early development, our AI framework offers a scalable platform that will require external validation before clinical deployment. Finally, the gene expression analysis was limited to a small cohort of patients, yet it provides a direction for future large-scale tissue transcriptomics evaluating IBD molecular signatures.

Looking ahead, future studies will aim to validate and refine our AI model across larger, diverse cohorts and explore its integration into prospective trial designs. Ultimately, we envision a next-generation, integrated framework for IBD assessment: the "endo-histo-barrier-OMICs approach."[9,10] Uniting AI-powered, high-resolution imaging (endo), histological evaluation (histo), functional barrier assessment (barrier), and multi-OMICs profiling (genomic, transcriptomic, proteomic, microbiome) offers the opportunity to map entotypes of barrier dysfunction and restoration trajectories in IBD. Such an approach holds the potential to transform patient stratification and establish barrier healing as a measurable and achievable treatment target in clinical practice.[26–31]

Acknowledgments

Endo-Histo-Barrier-Omics Group: Miguel Puga-Tejada,[1] Louise Burke,[2] Jane McCarthy,[3] Jennifer Morales,[4] for their substantial contributions in the successful completion of this study.

[1]APC Microbiome Ireland, College of Medicine and Health, University College Cork, Cork, Ireland; [2]Deparment of Pathology, University College Cork, Cork, Ireland; [3]Gastroenterology Unit, Mercy University Hospital, Cork; [4]APC Microbiome Ireland, Department of Anatomy and Neuroscience—School of Medicine, University College Cork, Cork, Ireland.

We would like to acknowledge IBD Nurses (Catherine O'Sullivan, Kathleen Sugrue, Cornelia Prendiville, Margot Hurley, and Anne-Marie O'Keeffe).

Author contributions

M.I.: study conception and design, data acquisition, analysis and interpretation of data, drafting of the manuscript, critical revision of the manuscript for important intellectual content, supervision. S.M.: data acquisition, analysis and interpretation of data, drafting of the manuscript, critical revision of the manuscript for important intellectual content. I.Z.: data acquisition, analysis and interpretation of data, drafting of the manuscript, critical revision of the manuscript for important intellectual content. G.S.: data acquisition, analysis and interpretation of data, drafting of the manuscript, critical revision of the manuscript for important intellectual content. I.C.: data acquisition, drafting of the manuscript, critical revision of the manuscript for important intellectual content. C.P.: data acquisition, drafting of the manuscript, critical revision of the manuscript for important intellectual content. U.C.: data acquisition, analysis and interpretation of data, critical revision of the manuscript for important intellectual content. P.M.: data acquisition, analysis and interpretation of data, critical revision of the manuscript for important intellectual content. B.H.: analysis and interpretation of data, critical revision of the manuscript for important intellectual content. R.C.: analysis and interpretation of data, critical revision of the manuscript for important intellectual content. M.A.: critical revision of the manuscript for important intellectual content. R.D.A.: analysis and interpretation of data, critical revision of the manuscript for important intellectual content. B.B.K.: critical revision of the manuscript for important intellectual content. J.E.: analysis and interpretation of data, critical revision of the manuscript for important intellectual content. A.A.: analysis and interpretation of data, critical revision of the manuscript for important intellectual content. V.N.: analysis and interpretation of data, critical revision of the manuscript for important intellectual content, supervision. E.G.: analysis and interpretation of data, critical revision of the manuscript for important intellectual content, supervision. S.G.: analysis and interpretation of data, critical revision of the manuscript for important intellectual content, supervision. All authors have contributed substantially to the acquisition or analysis of data and drafting of the manuscript and have approved the final version.

Supplementary material

Supplementary material is available at *ECCO-JCC* online.

Funding

Startup funds to M.I. from University College Cork (UCC), Ireland.

Conflicts of interests

No conflicts of interest to declare.

Data availability

Data are available from the corresponding author upon reasonable request.

References

1. Neurath MF, Vieth M. Different levels of healing in inflammatory bowel diseases: mucosal, histological, transmural, barrier and complete healing. *Gut*. 2023;72:2164-2183.
2. Sridhar S, Hart A, Venkat S, et al. P0061 Guselkumab induction therapy results in molecular resolution of inflammation in moderately to severely active Ulcerative Colitis: results from the Phase 3 QUASAR induction study. *J Crohns Colitis*. 2025;19:i421-i422.
3. Rath T, Atreya R, Bodenschatz J, et al. Intestinal barrier healing is superior to endoscopic and histologic remission for predicting major adverse outcomes in inflammatory bowel disease: the prospective ERIca trial. *Gastroenterology*. 2023;164:241-255.
4. Camilleri M. Leaky gut: mechanisms, measurement and clinical implications in humans. *Gut*. 2019;68:1516-1526. https://gut.bmj.com/lookup/doi/10.1136/gutjnl-2019-318427.
5. Zammarchi I, Santacroce G, Puga-Tejada M, et al. Epithelial neutrophil localization and tight junction Claudin-2 expression are innovative outcome predictors in inflammatory bowel disease. *United European Gastroenterol J*. 2024;12:1155-1166.
6. Spadoni I, Zagato E, Bertocchi A, et al. A gut-vascular barrier controls the systemic dissemination of bacteria. *Science*. 2015;350:830-834.
7. Iacucci M, Santacroce G, Majumder S, et al. Opening the doors of precision medicine: novel tools to assess intestinal barrier in inflammatory bowel disease and colitis-associated neoplasia. *Gut*. 2024;73:1749-1762.
8. Majumder S, Santacroce G, Maeda Y, et al. Endocytoscopy with automated multispectral intestinal barrier pathology imaging for assessment of deep healing to predict outcomes in ulcerative colitis. *Gut*. 2024;73:1603-1606.
9. Iacucci M, Maeda Y, Santacroce G, et al. AI-enabled 'endo-histo-omics': breaking down intestinal barriers in IBD. *Nat Rev Gastroenterol Hepatol*. 2025;22:362-363.
10. Iacucci M, Santacroce G, Zammarchi I, et al. Artificial intelligence and endo-histo-omics: new dimensions of precision endoscopy and histology in inflammatory bowel disease. *Lancet Gastroenterol Hepatol*. 2024;9:758-772. https://linkinghub.elsevier.com/retrieve/pii/S2468125324000530.
11. Iacucci M, Jeffery L, Acharjee A, et al. Computer-aided imaging analysis of probe-based confocal laser endomicroscopy with molecular labeling and gene expression identifies markers of response to biological therapy in IBD Patients: the endo-omics study. *Inflamm Bowel Dis*. 2023;29:1409-1420.
12. Yaseen Z, Gide TN, Conway JW, et al. Validation of an accurate automated multiplex immunofluorescence method for immuno-profiling melanoma. *Front Mol Biosci*. 2022;9:810858.
13. Lin S, Lin Y. Protocol for Freezing in OCT, *Protocols.Io*. 2020. https://doi.org/10.17504/protocols.io.bpx7mprn
14. Eng J, Bucher E, Hu Z, et al. A framework for multiplex imaging optimization and reproducible analysis. *Commun Biol*. 2022;5:438.
15. Bankhead P, Loughrey MB, Fernández JA, et al. QuPath: open source software for digital pathology image analysis. *Sci Rep*. 2017;7:16878.
16. Aeffner F, Zarella MD, Buchbinder N, et al. Introduction to digital image analysis in whole-slide imaging: a white paper from the Digital Pathology Association. *J Pathol Inform*. 2019;10:9.
17. Booth C, O'Shea JA. Isolation and culture of intestinal epithelial cells. In: *Culture of Epithelial Cells*. Wiley; 2002:303-335.
18. Kirchgesner J, Verstockt B, Adamina M, et al. ECCO topical review on predictive models on inflammatory bowel disease disease course and treatment response. *J Crohns Colitis*. 2025;19:jjaf073.
19. Turner D, Ricciuto A, Lewis A, et al. International Organization for the Study of IBD. STRIDE-II: an update on the Selecting Therapeutic Targets in Inflammatory Bowel Disease (STRIDE) Initiative of the International Organization for the Study of IBD (IOIBD): determining therapeutic goals for Treat-to-Target strategies in IBD. *Gastroenterology*. 2021;160:1570-1583.
20. Barbaro MR, Cremon C, Marasco G, et al. Molecular mechanisms underlying loss of vascular and epithelial integrity in irritable bowel syndrome. *Gastroenterology*. 2024;167:1152-1166.
21. Wang X, Memon AA, Palmér K, et al. The association of zonulin-related proteins with prevalent and incident inflammatory bowel disease. *BMC Gastroenterol*. 2022;22:3.
22. Górecka A, Jura-Półtorak A, Koźma EM, et al. Biochemical modulators of tight junctions (TJs): Occludin, Claudin-2 and Zonulin as biomarkers of intestinal barrier leakage in the diagnosis and assessment of inflammatory bowel disease progression. *Molecules*. 2024;29:4577.
23. Santacroce G, Zammarchi I, Tan CK, et al. Present and future of endoscopy precision for inflammatory bowel disease. *Dig Endosc*. 2024;36:292-304. https://onlinelibrary.wiley.com/doi/10.1111/den.14672.
24. Iacucci M, Santacroce G, Yasuharu M, et al. Artificial intelligence–driven personalized medicine: transforming clinical practice in inflammatory bowel disease. *Gastroenterology*. 2025;169:416-431.
25. Solitano V, Bernstein CN, Dotan I, et al. Shaping the future of inflammatory bowel disease: a global research agenda for better management and public health response. *Nat Rev Gastroenterol Hepatol*. 2025;22:438-452.
26. Iacucci M, Jeffery L, Acharjee A, et al. Ultra-high magnification endocytoscopy and molecular markers for defining endoscopic and histologic remission in ulcerative colitis—an exploratory study to define deep remission. *Inflamm Bowel Dis*. 2021;27:1719-1730.
27. Kiesslich R, Duckworth CA, Moussata D, et al. Local barrier dysfunction identified by confocal laser endomicroscopy predicts relapse in inflammatory bowel disease. *Gut*. 2012;61:1146-1153.
28. He K, Zhang X, Ren S, et al. Deep residual learning for image recognition. *2016 IEEE Conference on Computer Vision and Pattern Recognition (CVPR)*. IEEE; 2016:770-778. http://ieeexplore.ieee.org/document/7780459/.
29. Boers TGW, Fockens KN, Putten JAvd, et al. Foundation models in gastrointestinal endoscopic AI: Impact of architecture, pre-training approach and data efficiency. *Med Image Anal*. 2024;98:103298.
30. Iacucci M, Jeffery L, Acharjee A, et al. Computer-aided imaging analysis of probe-based confocal laser endomicroscopy with molecular labeling and gene expression identifies markers of response to biological therapy in IBD Patients: the endo-omics study. *Inflamm Bowel Dis*. 2023;29:1409-1420.
31. He K, Gkioxari G, Dollar P, et al. 2980-2988. Mask R-CNN. *2017 IEEE International Conference on Computer Vision (ICCV)*. IEEE; 2017.